Announcing the third generation of the Potsdam Magnetic Model of the Earth (POMME)

S. Maus

CIRES at the University of Colorado and NOAA's National Geophysical Data Center, Boulder, Colorado, USA

M. Rother, C. Stolle, W. Mai, S. Choi, and H. Lühr

GeoForschungsZentrum, Potsdam, Germany

C. Roth and D. Cooke

Air Force Research Laboratory, Hanscom Air Force Base, MA

Abstract. The Potsdam Magnetic Model of the Earth (POMME) is a geomagnetic field model providing an estimate of the Earth's core, crustal, magnetospheric and induced magnetic fields. The internal field is represented to spherical harmonic (SH) degree 90, while the secular variation and acceleration are given to SH degree 16. Static and time varying magnetospheric fields are parametrized in GSM and SM coordinates and include Dst-index and IMF-By dependent contributions. The model was estimated from five years of CHAMP satellite magnetic data. All measurements were corrected for ocean tidal induction and night-side ionospheric F-region currents. The model is validated using an independent model from a combined data set of Ørsted and SAC-C satellite measurements. For the core field to SH degree 13, the root mean square (RMS) vector difference between the two models at the center of the model period is smaller than 4 nT, when averaged over the Earth's surface. The RMS uncertainty increases to about 100 nT for the predicted field in 2010, as inferred from the difference between the two models.

1. Introduction

The recent satellite magnetic missions of Ørsted, CHAMP and SAC-C have provided the data basis for a new generation of highly accurate main field models [*Olsen et al.*, 2000; *Olsen*, 2002; *Holme et al.*, 2002; *Maus et al.*, 2005; *Lesur et al.*, 2005; *Olsen et al.*, 2006]. Typically, these models include

- A static internal field including core and crustal fields
- The secular variation
- The secular acceleration
- A time averaged magnetospheric field, including induction infects due to Earth rotation [*Maus and Lühr*, 2005]
- A time varying magnetospheric field, coupled to the Est/Ist index [*Maus and Weidelt*, 2004; *Olsen et al.*, 2005] and to the the Y-component of the interplanetary magnetic field [*Lesur et al.*, 2005]

In particular, seven years of continuous measurements have made it possible to determine the temporal derivatives of the core field in unprecedented accuracy.

2. Input data

There are presently three satellites with science quality magnetometers in low-Earth orbit: Ørsted, SAC-C and CHAMP. Ørsted scalar data is available with more than 80% coverage from 1999 to present, while Ørsted vector data has a coverage of nnn% and is only sporadically available since 2003. The vector magnetometer on SAC-C never provided accurate measurements, but its scalar magnetometer provided a data coverage of more than 70% from 2001 to the end of 2004. For CHAMP, scalar and vector data are almost continuously available since the start of the mission in mid 2000. The data used in this study are summarized in Table 2. Ørsted and SAC-C data were only used for an independent control model. Due to their large polar gap, lower quality and incomplete coverage, these data are less ideal for field modeling. The final POMME-3 model is therefore based solely on CHAMP data.

3. Data selection

We follow the data selection procedures which are generally used in main field modeling. For CHAMP data, we discard all tracks which were identified as being contaminated by magnetic signals due to plasma instabilities in the ionospheric F-region [*Stolle et al.*, 2005]. To reduce attitude uncertainty, CHAMP vector data are only used when the star-camera (SC) is in dual-head mode. Different criteria are applied to low- and high-latitude data. For the POMME model, high-latitude tracks cover the polar regions above 50° or below -50°, and low-latitude tracks cover the overlapping range of -60° to 60° magnetic latitude. The data selection criteria are summarized in Table 1. Finally, the tracks in all data sets were plotted in terms of RMS against longitude, and RMS against MJD, in order to identify and discard remaining tracks with abnormally high noise level.

0148-0227/06/$9.00

Table 2. Summary of vector and scalar measurements used in this study, where S.-polar tracks are below -50°, N.-polar are above 50°, and low-latitude tracks cover the overlapping range of -60° to 60° magnetic latitude. Also given is the time interval in Modified Julian Days (MJD) for which data are available. MJD zero is 1-Jan-2000. The right column gives the coverage of the raw data set during this period.

	S.-polar	low-latitude	N.-polar	MJD range	raw data coverage
CHAMP Vector		637,622		207 to 2069	94.2%
CHAMP Scalar	217,128	1,061,386	195,416	207 to 2068	95.5%
Ørsted Vector		423,511		-291 to 1651	44.4%
Ørsted Scalar	251,938	1,612,318	205,265	-291 to 2069	82.9%
SAC-C Scalar	156,063	850,472	138,602	388 to 1742	71.7%

Table 1. Summary of data selection criteria. Here, Kp and Dst are magnetic indices, and E_m is the merging electric field at the magnetopause.

	low latitude	high latitude
$Kp \leq 2$	√	√
3 hours earlier: $Kp \leq 2$	√	√
$\|Dst\| \leq 30$	√	√
$\|\partial_t\ Dst\| \leq 2$ nT/h	√	√
$\|IMF\text{-}By\| \leq 8$ nT		√
-2 nT $\leq$ IMF-Bz		√
$E_m \leq 0.8$ mV/m		√
21:00 $\leq$ LT $\leq$ 5:00	√	
CHAMP: dual-head SC mode	√	√
CHAMP: no plasma irregularities	√	

4. Data processing

Several corrections were applied to the data, namely for the mis-alignment of the CHAMP star camera (SC), for ambient plasma effects, and for ocean tidal induction.

4.1. Correction for CHAMP star camera misalignment

Every satellite vector-magnetometer requires an in-flight calibration of the angles between the coordinate systems of the SC and the vector magnetometer. For CHAMP, final level-3 data are not yet available and the level-2 data require the user to apply a SC misalignment correction. We regularly carry out the necessary calibration and distribute the calibration coefficients and software via the web site http://www.gfz-potsdam.de/pb2/pb23/Supplementals/index.html. All CHAMP vector data used in this study were corrected in this way.

4.2. Correction for ocean tidal magnetic fields

The ocean dynamo contributes with up to about 3 nT to the magnetic field measured at satellite altitude. This is a rather small effect. However, since it can be rather accurately predicted [*Kuvshinov and Olsen*, 2005], one may as well subtract this effect. We use the predictions of Kuvshinov, which are available at http://www.gfz-potsdam.de/pb2/pb23/SatMag/index_e.html.

4.3. Correction for diamagnetic effect

Pressure driven electric currents reduce the magnetic field in the ionospheric F-region by a few nanotesla. This effect is particularly important for CHAMP, with its orbital altitude close to the peak ionospheric plasma density. Using the electron density and temperature measurements from the Langmuir Probe, the magnetic field readings of CHAMP were corrected using the approximate formula for the diamagnetic effect given by *Lühr et al.* [2003]. For Ørsted and SAC-C similar corrections could be applied using an ionospheric model. However, since the effect is much smaller at their higher altitude, such a correction was not applied here.

4.4. Correction for gravity driven ionospheric currents

The gravity driven current system in the ionospheric F-region generates a significant magnetic signal of the order of 5 nT. In contrast to the pressure driven current, its magnetic signal is equally strong above and below the ionosphere. We therefore corrected the data of all three satellites for this effect. We take the densities from the International Reference Ionosphere, IRI-2000 [*Bilitza*, 2001], and determine the primary gravity-driven current on 46 horizontal shells with a vertical spacing of 20 km. For each shell, we then find the non-divergent, freely flowing part of the current. Integrating over the magnetic effects of the currents in all shells, we obtain the magnetic signal at the measurement locations along the satellite orbit. Further details of the correction are given in *Maus and Lühr* [2006].

5. Model parametrization and estimation

For the external magnetic field we used the model of *Maus and Lühr* [2005]. Such an external field model cannot be co-estimated from night-side-only data. We verified the published coefficient values on a new 24h data set of CHAMP and Ørsted data, finding such small differences that it was not justified to introduce an updated set of coefficients. Therefore, the new POMME model uses the values of the coefficients given in *Maus and Lühr* [2005] for the magnetospheric part of the geomagnetic field.

Following *Lesur et al.* [2005] and *Olsen et al.* [2006], we co-estimate a time-varying axial degree-1 external field in magnetic coordinates. A bin width of one day was chosen in order to prevent the aliasing of spatial effects, since a satellite covers the Earth with 15 orbits once in 24h. Of course, high-degree (n 7) fields could still alias into this external field estimate. The Dst index is known to have baseline problems and this co-estimate is known to improve the temporal derivatives of the internal field [*Lesur et al.*, 2005; *Olsen et al.*, 2006].

The internal field is parametrized in the usual way as

$$V(r,\vartheta,\varphi) = a\sum_{\ell=1}^{\infty}\left(\frac{a}{r}\right)^{\ell+1}\sum_{m=-\ell}^{\ell} g_\ell^m Y_\ell^m(\vartheta,\varphi), \qquad (1)$$

with the scalar potential V of the magnetic field, $\mathbf{B} = -\nabla V$, colatitude ϑ, longitude φ, degree ℓ, order m, magnetic reference radius $a = 6371.2$ km, and Gauss coefficients g_ℓ^m, where coefficients with negative order are sometimes denoted by h_ℓ^m. Finally, Y_ℓ^m are Schmidt semi-normalized spherical harmonics [*Backus et al.*, 1996].

Accounting for the change of the core field, each Gauss coefficient is given as a truncated Taylor expansion

$$g(t) = g + tg' + 0.5t^2 g''. \qquad (2)$$

The coefficients g were estimated to SH degree 60, while the secular variation g' and acceleration g'' were estimated to degree and order 16.

We used a direct solver for the least squares problem, via eigenvectors and eigenvalues of the normal equations. No regularization was applied to the Gauss coefficients of the static part of the field. For the secular variation, degrees 14-16 were damped to impose a decreasing spectrum of g', and degrees 10-16 of were damped to impose a decreasing spectrum of g''.

6. Result and discussion of accuracy

We estimate two models from (almost) independent data sets. One is from CHAMP data only, and the other is from the combined Ørsted and SAC-C data. However, due to the large polar gap of Ørsted and SAC-C we added some polar CHAMP data to their data set in order to avoid having to regularize the Ørsted/SAC-C model for the static field above SH degree 15. We also estimated a combined CHAMP/Ørsted/SAC-C model. However, this did not lead to an obvious improvement (as can be inferred from the noise level in the secular variation and acceleration) and we therefore decided to declare the CHAMP-only model as the new POMME.

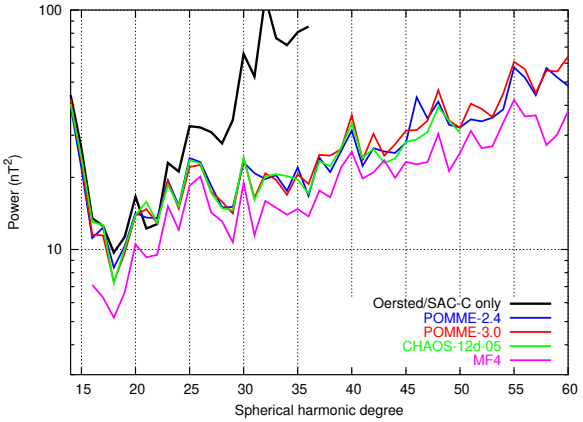

Figure 1. Power spectra of the static part of the internal field for our independent models from CHAMP (POMME-3.0) and from Ørsted/SAC-C data in comparison with the previous POMME-2.4 model, the CHAOS model [*Olsen et al.*, 2006], and the dedicated lithospheric field model MF4 [*Maus et al.*, 2006].

The power spectrum of the static part of the internal field is displayed in Figure 1. Shown are the CHAMP-only model (POMME-3.0), the combined Ørsted/SAC-C model, and two models which are not part of this study. One is the CHAOS model [*Olsen et al.*, 2006], and the other is the dedicated lithospheric field model MF4 [*Maus et al.*, 2006]. The spectra indicate a higher noise level of our Ørsted/SAC-C model, which is partly due to the higher orbital altitude of these two satellites. Furthermore, the spectra show a significantly lower power of MF4. This is due to the along-track filtering of the data used for MF4. The filter is designed to remove spurious long-wavelength external and induced fields but also removes some genuine lithospheric field. As can be seen from the spectra, the effect of contaminating external fields increases with increasing SH degree. Toward higher SH degrees a model from filtered data, such as MF4, is therefore preferable over a model from unfiltered data.

Figure 2 shows the power spectra of the secular variation and secular acceleration. All three models shown here are damped. These spectra therefore do not provide much information on the accuracy of the models.

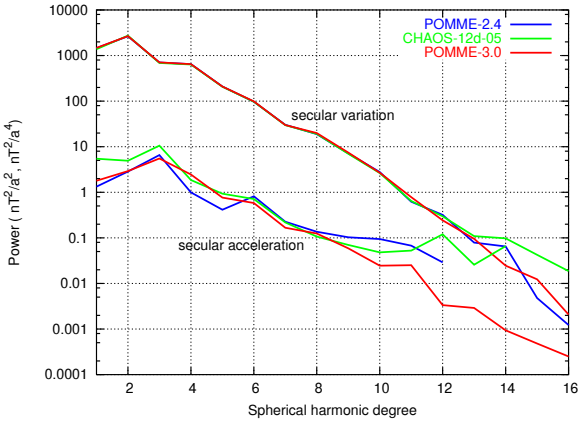

Figure 2. Power spectra of the first and 2nd time derivative of the internal field for the new POMME-3.0 model from CHAMP data, in comparison with the previous POMME-2.4, and with the new CHAOS model by *Olsen et al.* [2006]. The time derivatives of all three models are damped.

Finally, the inversion included the co-estimation of a time-varying, axial, degree-1 external field (q_1^0) in magnetic coordinates. These fields can be interpreted as inaccuracies of the Dst index. The time series of q_1^0 for the two models is given in Figure 3. The magnitude of the result is realistic, and the agreement between the two models shows that these fields are real. Disagreements with a period of 110 days between the two curves are probably due to local-time differences between CHAMP and the other two satellites, which sample the asymmetric ring-current field in varying local time sectors. In contrast to the CHAOS model, we did not co-estimate q_1^1 and q_1^{-1} because our external field already includes time-varying q_1^1 and q_1^{-1} fields correlated with the IMF-By.

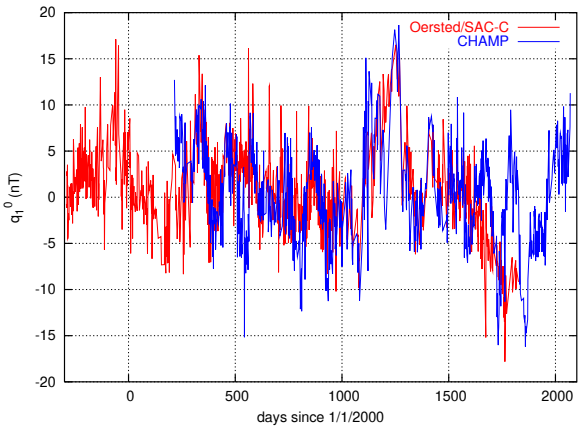

Figure 3. Time series of the offsets in the external, uniform field (q_1^0), aligned with the magnetic dipole. The estimates from CHAMP and from Ørsted/SAC-C data agree rather well. Differences are mostly due to the asymmetry of the external field, sampled by the satellites in different local time orbits.

For an estimate of model uncertainty, we directly compare our CHAMP and Ørsted/SAC-C models for the inter-

nal field to SH degree 13 at the Earth's surface. Figure 4 shows a map of the difference in the vertical component in 2002. The difference is rather equally distributed over the Earth's surface and there is no indication of a systematic error in one of the models. For an estimate of the reliability of the secular variation estimates, we apply the secular variation and acceleration up to SH degree 13 to both models and compute the RMS vector difference at the Earth's surface from 1995 to 2010, shown in Figure 5. As expected, the models agree best in the period during which data are present for both models. The optimum agreement is confined to the time of simultaneous availability of vector data from 2000.5 to 2003.5. The RMS difference between the two models increases to about 100 nT for the predicted core field in 2010. This figure of 100 nT provides an estimate of the uncertainty of the prediction, assuming that the behavior of the core field is entirely determined by its secular variation and acceleration. An additional uncertainty arises from possible changes in the secular acceleration of the field. Such sudden changes in the secular acceleration are visible in ground magnetic observatory records and are generally referred to as jerks.

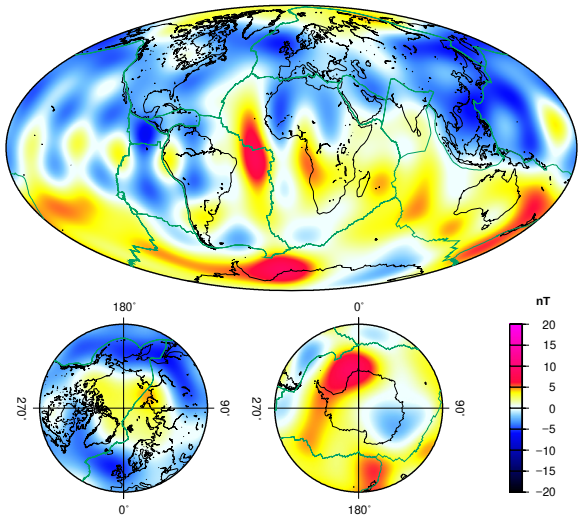

Figure 4. Map of the difference between our independent models from CHAMP and from Ørsted/SAC-C data, the former minus the latter. Displayed is the difference in the z-component at the Earth's surface.

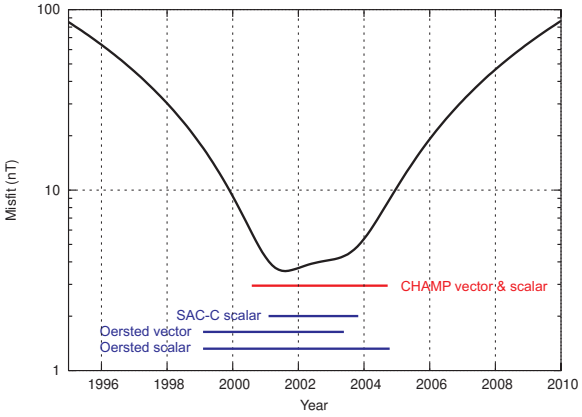

Figure 5. RMS vector difference at the Earth's surface between our independent models from CHAMP and from Ørsted/SAC-C data, for the time period from 1995 to 2000. The models were evaluated to SH degree 13, including the secular variation and acceleration to the same SH degree.

7. Model availability

The model estimated from CHAMP data is declared as POMME-3.0. For high internal SH degrees, a superior representation of the field is given by the dedicated lithospheric field model MF4 [*Maus et al.*, 2006], which was also produced only from CHAMP data. We therefore merge degrees 1 to 24 of POMME-3.0 with degrees 25 to 90 of MF4 to produce the final model POMME-3.1. The spectra of these models are shown in Figure 6. The coefficients of POMME-3.0 and POMME-3.1, together with software in the languages C, Matlab and IDL to evaluate the models is available from our web sites http://geomag.colorado.edu/pomme3.html and http://www.gfz-potsdam.de/pb2/pb23/SatMag/pomme3.html. The Ørsted/SAC-C model, which was derived here solely for the purpose of verifying the accuracy of POMME-3.0, is available on request.

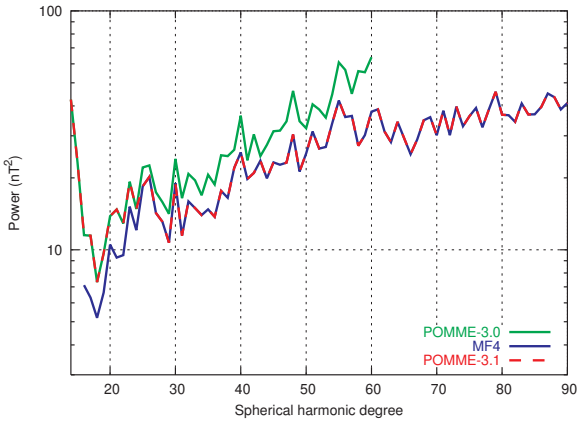

Figure 6. Spectra of the POMME-3.0 and the MF4 models. The POMME-3.1 model, spectrum overlaid as a dashed line, was constructed by merging the lower-degree portion of POMME-3.0 with the higher-degree portion of MF4. The degree at which the models were merged was chosen rather arbitrarily, since it is not evident at which SH degree the merit of filtering the data begins to dominate over the accompanying loss of genuine lithospheric signal.

Acknowledgments. The operational support of the CHAMP mission by the German Aerospace Center (DLR) and the financial support for the data processing by the Federal Ministry of Education and Research (BMBF) are gratefully acknowledged. The Ørsted and SAC-C projects received extensive support from the Danish government, the Argentine Commission on Space Initiatives, NASA, ESA, CNES and DARA.

References

Backus, G., R. L. Parker, and C. Constable, *Foundations of Geomagnetism*, Cambridge Univ. Press, 1996.

Bilitza, D., International Reference Ionosphere 2000, *Radio Science*, *36*, 261–275, 2001.

Holme, R., N. Olsen, M. Rother, and H. Lühr, *CO2 - A CHAMP magnetic field model*, pp. 220–225, CHAMP Mission Results I, Springer Berlin, 2002.

Kuvshinov, A., and N. Olsen, *3-D modelling of the magnetic field due to ocean tidal flow*, pp. 359–365, Springer, Berlin - Heidelberg, 2005.

Lesur, V., S. Macmillan, and A. Thomson, A magnetic field model with daily variations of the magnetospheric field and its induced counterpart in 2001, *Geophys. J. Int.*, *160*, 79–88, doi: 10.1111/j.1365-246X.2004.02479.x, 2005.

Lühr, H., M. Rother, S. Maus, W. Mai, and D. Cooke, The diamagnetic effect of the equatorial Appleton anomaly: Its characteristics and impact on geomagnetic field modeling, *Geoph. Res. Lett.*, *30*(17), 10.1029/2003GL017,407, 2003.

Maus, S., and H. Lühr, Signature of the quiet-time magnetospheric magnetic field and its electromagnetic induction in the rotating Earth, *Geophys. J. Int.*, doi:10.1111/j.1365-246X.2005.02691.x, 2005.

Maus, S., and H. Lühr, A gravity-driven electric current in the Earth's ionosphere identified in CHAMP satellite magnetic measurements, *Geophys. Res. Lett.*, *in print*, 2006.

Maus, S., and P. Weidelt, Separating the magnetospheric disturbance magnetic field into external and transient internal contributions using a 1D conductivity model of the Earth, *Geophys. Res. Lett.*, *31*, L12,614, 10.1029/2004GL020,232, 2004.

Maus, S., H. Lühr, G. Balasis, M. Rother, and M. Mandea, Introducing POMME, Potsdam Magnetic Model of the Earth, in *Earth Observation with CHAMP: Results from Three Years in Orbit*, edited by C. Reigber, H. Lühr, P. Schwintzer and J. Wickert, pp. 293–298, Springer, Berlin - Heidelberg, 2005.

Maus, S., M. Rother, K. Hemant, C. Stolle, H. Lühr, A. Kuvshinov, and N. Olsen, Earth's crustal magnetic field determined to spherical harmonic degree 90 from CHAMP satellite measurements, *Geophys. J. Int., under revision*, *164*, 319–330, doi:doi:10.1111/j.1365-246X.2005.02833.x, 2006.

Olsen, N., A model of the geomagnetic main field and its secular variation for epoch 2000 estimated from Ørsted data, *Geophys. J. Int.*, *149*, 454–462, 2002.

Olsen, N., T. J. Sabaka, and F. Lowes, New parameterization of external and induced fields in geomagnetic field modeling, and a candidate model for IGRF 2005, *Earth Planets Space*, *57*(12), 1141–1149, 2005.

Olsen, N., H. Lühr, T. J. Sabaka, M. Mandea, M. Rother, L. Tøffner-Clausen, and S. Choi, CHAOS - a model of Earth's magnetic field derived from CHAMP, ørsted, and SAC-C magnetic satellite data, *Geophys. J. Int.*, *submitted*, 2006.

Olsen, N., et al., Ørsted initial field model, *Geophys. Res. Lett.*, *27*, 3607–3610, 2000.

Stolle, C., H. Lühr, and M. Rother, Magnetic signatures of equatorial plasma bubbles as observed by the CHAMP satellite, *J. Geophys. Res.*, submitted, 2005.

S. Maus, Stefan Maus, National Geophysical Data Center, NOAA E/GC1, 325 Broadway, Boulder, CO 80305-3328, USA, email: Stefan.Maus@noaa.gov

M. Rother, GeoForschungsZentrum, Telegrafenberg, D-14473 Potsdam, Germany, email: rother@gfz-potsdam.de